

# A New Five Wheeled Rover for All Terrain Navigation

Arun H Patil<sup>1</sup>, Arun Kumar Singh<sup>1</sup>, Dr. Anup Kumar Saha<sup>1\*</sup>

<sup>1</sup>Mechanical Engineering Department, National Institute of Technology Durgapur, Durgapur, India  
\*Corresponding author (saha\_ak2001@yahoo.co.in)

## Abstract

This paper describes a new suspension concept for rough terrain navigation of rovers. The proposed design has reduced number of joints and links from the existing suspension concepts. The suspension mechanism is derived from planar four bar mechanism and hence we present the coupler curve trajectory as well as singularity analysis. We derive the quasi-static equation of motion of the vehicle and a linear programming approach is proposed for optimum wheel motor torques control. We test the proposed concept by extensive simulations on undulating terrains as well as on terrains having discontinuities.

**Keywords:** Four bar mechanism, singularity, linear programming, and dynamics.

## 1 Introduction

To design an effective suspension mechanism with minimum design and control complexity is the focus of the research here. Past research on wheeled all terrain vehicles has led to the development of two types of suspension mechanisms: active and passive. Passive suspension rovers adapt passively to the underlying by the virtue of contact forces and hence do not require any actuators for controlling the internal configuration of the vehicle thus significantly reducing the control architecture. Rocky7 [1] is one such vehicle which utilizes one of the most simplest suspension mechanisms called rocker bogie. But the climbing ability and specially the lateral stability is limited as compared to shrimp[2] which utilizes a more sophisticated design derived from the four bar mechanism to enhance climbing ability. But as sophistication increases the number of joints and links also increases significantly increasing the overall complexity and weight of the system. . In general joints are heavy parts and can easily lead to trouble in space environments [3]. Passive suspension rovers are usually multi wheel drive system [MWD] e.g. some rovers such as Lunokhod [4] and Marshakhod [5] have 6 or more wheels. Though the system has higher degree of mobility the system is intended to be heavier and hence not ideally applicable to medium to small scale rovers. Moreover the closed kinematic structures of passive

suspension rovers pose additional constraint on the kinematic analysis and motion planning robot. Hence the aim of this paper is to significantly reduce the kinematic complexity by reducing the number of joints and closed loops but without compromising with the climbing ability of the, on the other hand active suspension rovers are kinematically simple but employs complex control architectures to command the actuators controlling the internal configuration of the rover. These control architectures critically depend on number of sensor inputs which can be easily corrupted by noise in uncertain environments. Owing to this reason the focus of the research here is concentrated passive suspension with an aim to reduce the overall complexity of the design while maintaining the same obstacle climbing ability. We present the trajectory and singularity analysis of the mechanism proposed and a wheel motor torque control technique under quasi-static conditions. Efficacy of the proposed suspension is proven by extensive simulation on rough terrains.

## 2. Kinematic model of the rover

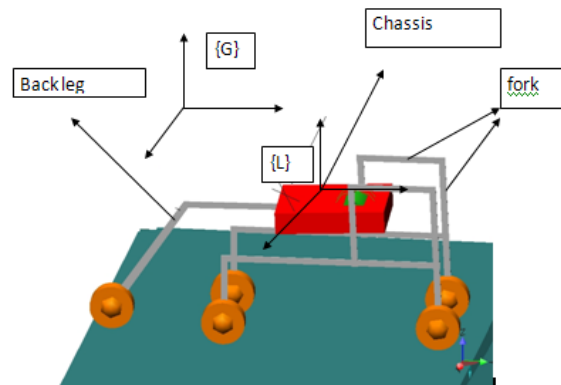


Fig.1: Kinematic model

The kinematic mode of the rover is shown in figure1. It consists of two planar mechanisms on two sides of the chassis. The front wheel on both sides is connected to the end of the fork which is derived from the four bar mechanism. The common back leg is attached to the chassis through some compliance in the form of rotational joint passively controlled by torsion spring of high spring constant. This is one of the novelties of the design

because unlike other designs such as [2] where back leg is directly connected by rigid joint, we introduce some compliance between the back leg and the wheel. This modification allows the rover to have some level of adaptivity on uneven terrains even while moving backward. The other important novelty of the proposed design is the reduction in number of joints and links. The Planar view of the robot with its joints is shown in figure 2.

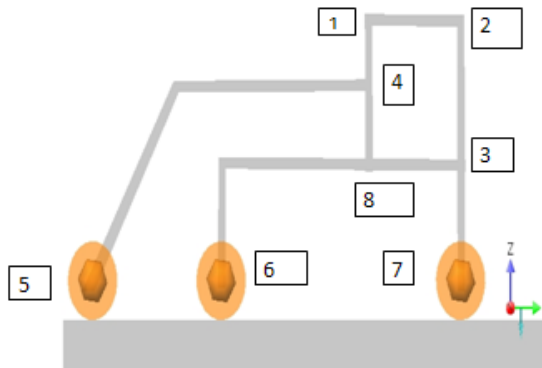


Fig. 2: Front view of the rover

All designated joints are revolute with 5, 6, 7 being the actuated joint for driving the wheels and joint 4 being controlled by passive joint. The number of joints is 16 in total and number of bodies (excluding ground) is 15. A similar functioning design found in [2] employs 18 bodies and 22 joints. Joints are generally heavier and critical part because they have maximum tendency of failing and hence corresponding decrease of the number of joints in the proposed design not only reduces the overall weight of the system but also increases the reliability of the system.

### 3 Kinematics of Fork

The fork with its geometrical parameters are shown in fig4

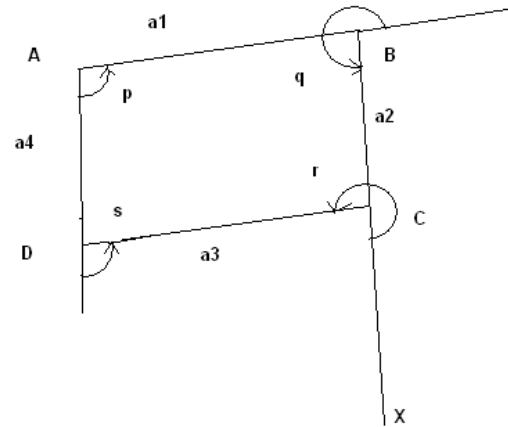


Fig. 3: Geometry of fork

We are interested in finding out the trajectory of point X as the link AB is rotated to a particular angle. This simulates the situation encountered while the front fork is climbing the obstacle. We analyze the optimisable parameters from the trajectory plot of X. To generate the trajectory of point X considering joint A to be the input angle we derive the two loop closure equations for the four bar mechanism ABCD following the work of [6] and is briefly reviewed here. Consider the four bar mechanism to be broken at point C which will result in two planar 2R and 1R serial kinematic chain. This is shown in figure 4. In the figure (x,y) represents the co-ordinates of coupler point X

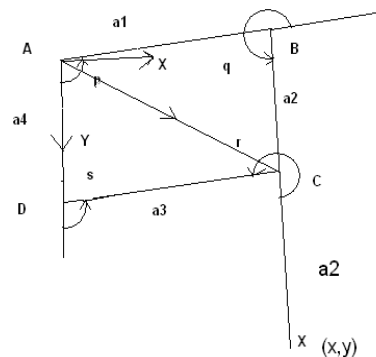


Fig. 4: Breaking the mechanism at point C

Since the mechanism has been broken at point C passive variable C will not appear in the loop closure constraint equation.

We have from figure3

$$y = a1 \cos(p) + 2a2 \cos(p+q) \dots\dots\dots(1)$$

$$x = a1 \sin(p) + 2a2 \sin(p+q) \dots\dots\dots(2)$$

$$y = a3 \cos(s) + a2 \cos(p+q) \dots\dots\dots(3)$$

$$x = a3 \sin(s) + a2 \sin(p+q) \dots\dots\dots(4)$$

$$y = -a1 \cos(p) + a2 \cos(p+q) = a4 + a3 \cos(s) + a2 \cos(p+q) \dots\dots(5)$$

$$x = a1 \sin(p) + a2 \sin(p+q) = a3 \sin(s) + a2 \sin(p+q) \dots\dots\dots(6)$$

from equation (5) and (6) we can eliminate the passive variables q, s and get x and y as a function of active joint variable p

We solve equation (5) and (6) using non linear methods such as Newton's method. The deduced trajectory of point X is shown in figure 5.

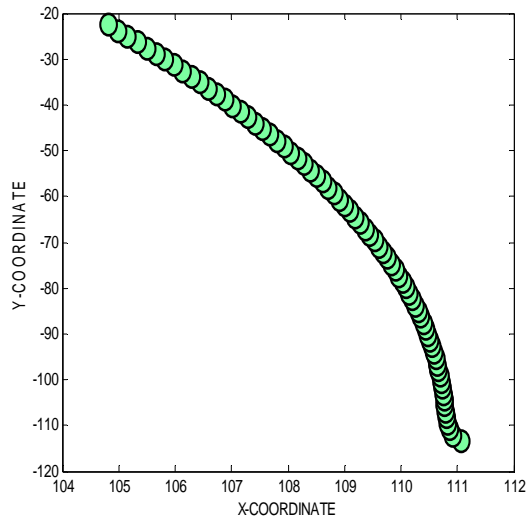


Fig.5: Trajectory of point X of fork

From the graph we can see that between the range of -110 to -90 there is little change in x coordinate as compared to y coordinate. This means that during this range the fork approximately follows a vertical straight line. This range of 20 cm is twice the wheel diameter. The advantage of vertical trajectory becomes critical while climbing discontinuities having slopes in the region of 90° because the angle between the allowed direction of motion of the fork and the traction forces resulting from the obstacle is 0° which allows the effective utilization of traction force while climbing over the obstacle.

### 4 Singularities of the Fork

A singularity analysis of the fork will enable us to make provision for its prevention by incorporating some mechanical stoppers at those positions to prevent the mechanism from reaching that state. To derive the point of singularity we follow the work of [6]. We have from

equation (5) and (6)

$$\eta = -a1 \cos(p) + a2 \cos(p+q) - a4 - a3 \cos(s) = 0 \dots\dots\dots(7)$$

$$\eta = a1 \sin(p) + a2 \sin(p+q) - a3 \sin(s) = 0 \dots\dots\dots(8)$$

In equation (7) and (8) we have q and s as passive variables and p as active variables. Differentiating both the equations with respect to time and writing them in matrix form yields

$$\begin{bmatrix} a1 \sin(p) - a2 \sin(p+q) \\ a1 \cos(p) + a2 \cos(p+q) \end{bmatrix} \left( \frac{d(p)}{dt} \right) + \begin{bmatrix} -a2 \sin(p+q) a3 \sin(s) \\ a2 \cos(p+q) - a3 \cos(s) \end{bmatrix} \left[ \left( \frac{dq}{dt} \right) \right] = 0 \dots\dots(9)$$

Let

$$K = \begin{bmatrix} a1 \sin(p) - a2 \sin(p+q) \\ a1 \cos(p) + a2 \cos(p+q) \end{bmatrix}$$

$$*K = \begin{bmatrix} -a2 \sin(p+q) a3 \sin(s) \\ a2 \cos(p+q) - a3 \cos(s) \end{bmatrix}$$

The singular positions can be found by equation

$$\det[*K] = 0 \dots\dots\dots(10)$$

which reduces to

$$a2 a3 \cos(s) \sin(p+q) - a2 a3 \cos(p+q) \sin(s) = 0 \dots\dots\dots(11)$$

$$a2 a3 \sin(p+q-s) = 0 \dots\dots\dots(12)$$

Or

$$p+q-s = n\pi, n=1 \dots\dots\dots(13)$$

Also from figure 3 we have

$$p+q+r+(\pi-s) = 4\pi \dots\dots\dots(14)$$

So

$$r = 2\pi \dots\dots\dots(15)$$

Which means that the link 2 and 3 are parallel or B,C,D are in straight line. This can be prevented by adding a stopper a joint C which will allow for the restricted rotation of joint.

### 5 Dynamics of the rover

In this section we prepare a dynamic model of the rover and solve the inverse dynamics problem where the velocity, acceleration and the orientation of the chassis is given and we are required to compute the feasible set of motor torques that can be applied to this system under equilibrium and no-slip constraints. In real life situations velocity, acceleration and orientation of the chassis can be easily determined from sensors such as accelerometers and gyroscopes. At the wheel ground contact point two sets of forces are acting, normal and traction forces as shown in figure6

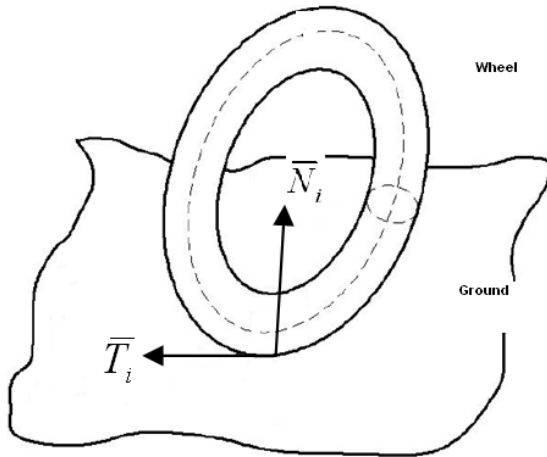


Fig6 forces at the wheel ground contact point

We assume that the normal force unit vectors are known. This is a valid assumption if the rover is equipped with tactile wheels as proposed in [7]. The traction force can be calculated by the methodology proposed in [8]. Let  $p, q$  and  $r$  be the pitch, roll and yaw angles respectively of the chassis about the global  $\{G\}$  axes. The local and global frames ( $\{L\}, \{G\}$ ) are shown in figure1 respectively. The resultant rotation matrix relating position vectors and the force components at various points to the reference frame of the chassis is:

$$R = R_z(q)R_y(r)R_x(p) \dots \dots \dots (16)$$

Where  $R_x(\psi)$ ,

$R_y(\alpha)$  and  $R_z(\beta)$  are the rotation matrices corresponding to the Euler angles about the  $X, Y$  and  $Z$  axes respectively

From Fig.6 the forces acting at the  $i^{th}$  wheel of the vehicle from the chassis (Local frame  $\{L\}$ ) reference frame are

- i) The normal force  $\vec{N}_{iL} = [N_{xi} \ N_{yi} \ N_{zi}]^T$
- ii) The traction force  $\vec{T}_{iL} = [T_{xi} \ T_{yi} \ T_{zi}]^T$

We assume that the motion of the vehicle to be non-holonomic in nature i.e the velocity of the vehicle along the direction perpendicular to the wheels is negligible. This is shown to be satisfied in the results and simulations section. and hence from the chassis reference frame we have

$$T_{xi} \approx 0 \text{ and } T_{yi} > 0.$$

Under no slip conditions we have  $|\vec{T}_{iL}| \leq \mu_i |\vec{N}_{iL}| \quad \forall i \in \{1, 2, 3, 4, 5\} \dots \dots \dots (17)$

Where  $\mu_i$  is the coefficient of friction between the point of contact of  $i^{th}$  wheel and the terrain.

Since  $\vec{T}_{iL}$  is always perpendicular to  $\vec{N}_{iL}$  we have

$$\begin{aligned} \text{dot}(\vec{T}_{iL}, \vec{N}_{iL}) &= 0 \\ \Rightarrow \\ N_{xi}T_{xi} + N_{yi}T_{yi} + N_{zi}T_{zi} &= 0 \dots \dots \dots (18) \end{aligned}$$

From (17)

$$\begin{aligned} |\vec{T}_{iL}| &= \eta \mu_i |\vec{N}_{iL}| \quad \Rightarrow \\ T_{xi}^2 + T_{yi}^2 + T_{zi}^2 &= (\eta \mu_i)^2 N_{iL}^2 \dots \dots \dots (19) \end{aligned}$$

Where  $0 < \eta \leq 1$

If  $|\vec{N}_{iL}| \neq 0$  then any one of the components

$N_{xi}, N_{yi}, N_{zi} \neq 0$ , In general  $N_{zi} \neq 0$ , as long as the wheels remain in contact, then from (18) and (19) we get

$$(\eta \mu_i)^2 |\vec{N}_{iL}|^2 - T_{xi}^2 = T_{yi}^2 + \left[ \frac{N_{xi}T_{xi} + N_{yi}T_{yi}}{N_{zi}} \right]^2 \dots \dots \dots (20)$$

Simplifying the above we get in the form:

$$aT_{yi}^2 + bT_{yi} + c = 0 \dots \dots \dots (21)$$

Solving the above quadratic equation we get

$$T_{yi} = \frac{\eta \mu_i |\vec{N}_{iL}| |N_{zi}|}{\sqrt{N_{zi}^2 + N_{yi}^2}} \quad \text{and} \quad T_{zi} = \frac{-\eta \mu_i N_{yi} |\vec{N}_{iL}| |N_{zi}|}{N_{zi} \sqrt{N_{zi}^2 + N_{yi}^2}}$$

Now the unit vectors of  $\vec{T}_{iL}$  and  $\vec{N}_{iL}$  in the global reference frame are

$$\hat{t}_i = R \frac{\vec{T}_{iL}}{|\vec{T}_{iL}|} = [t_{xi} \ t_{yi} \ t_{zi}]^T \dots \dots \dots (22)$$

and

$$\hat{n}_i = R \frac{\vec{N}_{iL}}{|\vec{N}_{iL}|} = [n_{xi} \ n_{yi} \ n_{zi}]^T \dots \dots \dots (23)$$

Where  $\vec{T}_i = R\vec{T}_{iL}$  and  $\vec{N}_i = R\vec{N}_{iL}$  are the traction and normal forces at the point contact in the global reference frame.

To get the arm vectors we use the following procedure. We get the vector connecting the wheel ground contact point to the centre of the chassis by first considering a planar view of the mechanism and then multiplying the arm vector hence derived with the rotation matrix combining the roll and yaw angles. This is exemplified by figure7 which shows the planar view of the suspension which is nothing but the projection of the suspension in the pitch plane.

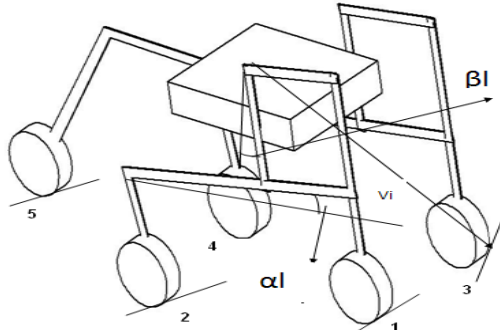


Fig7 orientation on arbitrary terrain

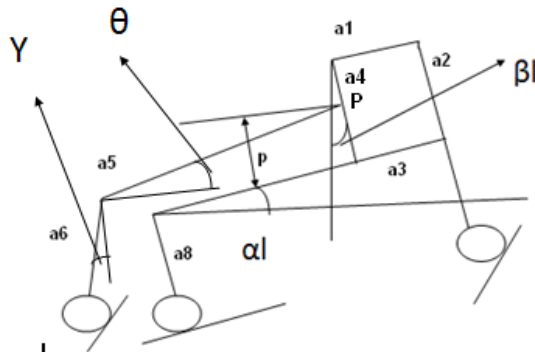


Fig.8: Planar projections of the suspension mechanism

As shown in figure7 P represents the point of attachment of the chassis. Vi represents the radius vector from the centre of the mass to the wheel ground contact point of the ith wheel. The planar projection showing the link and geometrical parameters are shown in figure8. It is to be noted that the first four wheels are symmetrical with each other. So the link parameters for the front part of the suspensions are same.  $\alpha l$  and  $\beta l$  are the angles made by the corresponding links on the front and back b side of the suspension mechanism and. The radius vector of the wheels in the pitch plane are given by the following expression

$$V1x = a1 \sin(\alpha l) - a2 \sin(\beta l) \dots \dots \dots (24)$$

$$V1y = a2 \cos(\beta l) - p \cos(\beta l) - a1 \sin(\alpha l) \dots \dots \dots (25)$$

$$V2x = a4 \sin(\beta l) + a7 \cos(\alpha l) - a8 \sin(\alpha l) \dots \dots \dots (26)$$

$$V2y = a8 \cos(\alpha l) + a7 \sin(\alpha l) - a8 \sin(\alpha l) \dots \dots \dots (27)$$

$$V3x = a1 \sin(\alpha r) - a2 \sin(\beta r) \dots \dots \dots (28)$$

$$V3y = a2 \cos(\beta r) - p \cos(\beta r) - a1 \sin(\alpha r) \dots \dots \dots (29)$$

$$V4x = a4 \sin(\beta r) + a7 \cos(\alpha r) - a8 \sin(\alpha r) \dots \dots \dots (30)$$

$$V4y = a8 \cos(\alpha r) + a7 \sin(\alpha r) - a8 \sin(\alpha r) \dots \dots \dots (31)$$

$$V5x = a5 \cos(\theta) + a6 \sin(\gamma) \dots \dots \dots (31a)$$

$$V5y = a5 \sin(\theta) + a6 \cos(\gamma) \dots \dots \dots (31b)$$

The radius vectors in the global reference frame are given by

$$r_i \hat{a}_i = R_z(\beta) R_y(\alpha) \begin{bmatrix} Vix \\ Viy \\ 0 \end{bmatrix} + R_z \begin{bmatrix} (25-i)H \\ (25-i)W \\ 0 \end{bmatrix} (-1)^{i+1} + r \begin{bmatrix} \hat{n}_ix \\ \hat{n}_iy \\ \hat{n}_iz \end{bmatrix} \quad \forall i \in \{1,2,3,4,5\}$$

where H and W are the width and depth of the chassis in global x and z direction respectively, r represents the wheel radius and  $\hat{n}_ix, \hat{n}_iy, \hat{n}_iz$  represents the unit vector f normal forces in the global frame

Let  $[m_{ixi} \ m_{iyi} \ m_{izi}]^T, [m_{nxi} \ m_{nyi} \ m_{nzi}]^T$  be the unit moment vectors due to  $\vec{T}_i$  and  $\vec{N}_i$  respectively.

Hence the quasi-static equations that relate the normal and traction forces to the forces on the chassis of a three dimensional (3D) suspension vehicle can be put in the form:

$$\bar{A} \bar{C} = \bar{D} \dots \dots \dots (32)$$

where

$$\bar{C} = [|\vec{T}_1| \ |\vec{N}_1| \ |\vec{T}_2| \ |\vec{N}_2| \ |\vec{T}_3| \ |\vec{N}_3| \ |\vec{T}_4| \ |\vec{N}_4|]^T$$

$$\bar{D} = [F_x \ F_y \ F_z \ M_x \ M_y \ M_z]^T$$

$$\bar{A} = \begin{bmatrix} t_{netx1} & n_{netx1} & t_{netx2} & n_{netx2} & t_{netx3} & n_{netx3} & t_{netx4} & n_{netx4} & t_{netx5} & n_{netx5} \\ t_{nety1} & n_{nety1} & t_{nety2} & n_{nety2} & t_{nety3} & n_{nety3} & t_{nety4} & n_{nety4} & t_{nety5} & n_{nety5} \\ t_{netz1} & n_{netz1} & t_{netz2} & n_{netz2} & t_{netz3} & n_{netz3} & t_{netz4} & n_{netz4} & t_{netz5} & n_{netz5} \\ m_{ix1} & m_{nx1} & m_{ix2} & m_{nx2} & m_{ix3} & m_{nx3} & m_{ix4} & m_{nx4} & m_{ix5} & m_{nx5} \\ m_{iy1} & m_{ny1} & m_{iy2} & m_{ny2} & m_{iy3} & m_{ny3} & m_{iy4} & m_{ny4} & m_{iy5} & m_{ny5} \\ m_{iz1} & m_{nz1} & m_{iz2} & m_{nz2} & m_{iz3} & m_{nz3} & m_{iz4} & m_{nz4} & m_{iz5} & m_{nz5} \end{bmatrix}$$

The above set of equations are under-constrained in the sense that they have more number of variables than equations. To reach a unique solution we solve the following optimization problem

$$\min(S) \dots \dots \dots$$

$$S = \sum_{i=1}^4 |\vec{T}_i| \dots \dots \dots (33)$$

Subjected to the following constraints

$$|\vec{N}_i| \geq 0 \quad \forall i = \{1, 2, 3, 4, 5\} \dots \dots \dots (34)$$

$$|\vec{T}_i| \leq \mu_i |\vec{N}_i| \quad \forall i = \{1, 2, 3, 4, 5\} \dots \dots \dots (35)$$

$$\Gamma_i^{\min} \leq (|\vec{T}_i| \cdot r) \leq \Gamma_i^{\max} \quad \forall i = \{1, 2, 3, 4, 5\} \dots \dots \dots (36)$$

Where (34) corresponds to the constraint that the wheel maintains contact with the ground always, (35) corresponds to the no-slip constraint and (36) corresponds to the constraint that the torque required to generate the required traction is between  $\Gamma_i^{\min}$  and  $\Gamma_i^{\max}$

## 6 Simulations and Results

Simulations were performed using Matlab and Msc Visual Nastran. Extensive simulations on uneven terrain for both 5-wheeled. Maximum coefficient of friction and maximum torque requirement were selected as the major parameters for comparison between the mechanisms. We set the maximum permissible torque of the motor at 4N-m. The coefficient of friction between the wheel and terrain was varied and minimum co-efficient of friction required to overcome the given terrain was noted for the proposed suspension mechanism. Figure9 shows 5-wheeled rover climbing a terrain with 70<sup>0</sup> degree discontinuity about two times the wheel diameter. The plot of the wheel motor torques is shown in figure10.

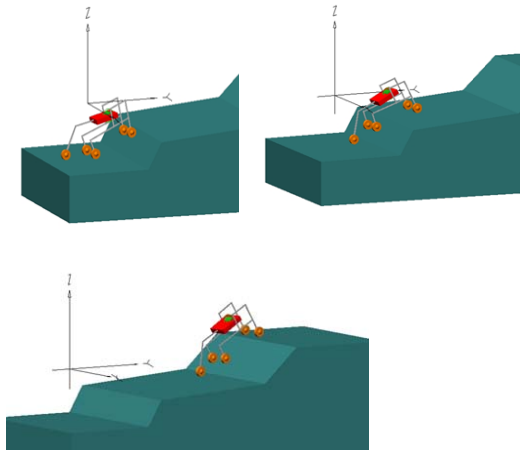
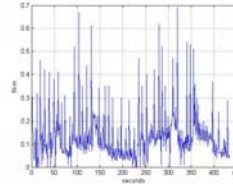
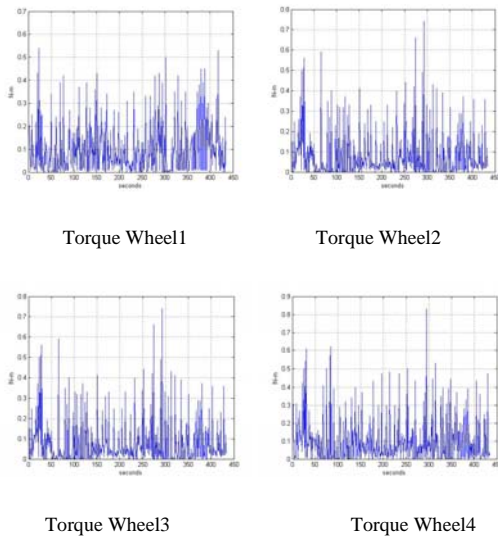


Figure9: 5-wheeled rover climbing a sample terrain



Torque Wheel5

Figure.10: wheel torques in N-m

As can be seen from figure10 the maximum torque reading comes out to be around 0.8 N-m when the fourth wheel is climbing the obstacle. The coefficient of friction between the wheel and the terrain was kept at 0.5 which was to be found to be the minimum for the rover to climb over the given terrain. Figure11 shows the satisfaction of the non-holonomic constraint i.e the rover's velocity along the direction perpendicular to the wheel is shown to be negligible in the plot which justifies our assumption that  $T_{xi} \approx 0$

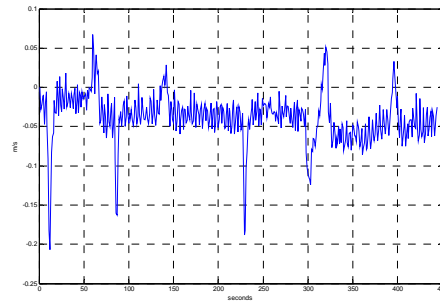
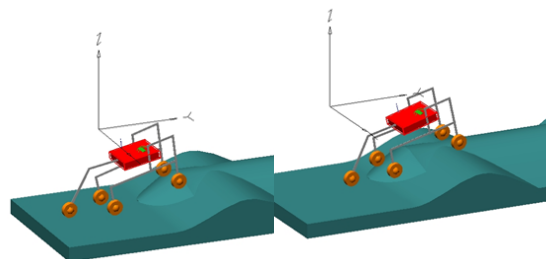


Figure11 Vx chassis from body coordinate frame

Figure 12 shows the 5-wheeled rover traversing on a fully 3D terrain which has slopes in all three orthogonal directions. The minimum coefficient of friction requirement for this terrain went up to 0.7. The increment in the requirement of the coefficient of friction was to ensure minimum lateral slippage of the wheels since the terrain also includes lateral slopes. The plot of wheel motor torques for the terrain is shown in figure13.



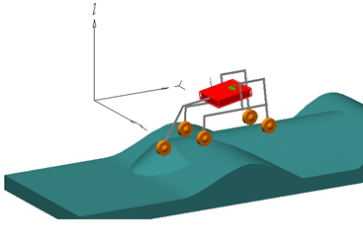


Figure.12: 5-wheeled rover climbing a 3D terrain

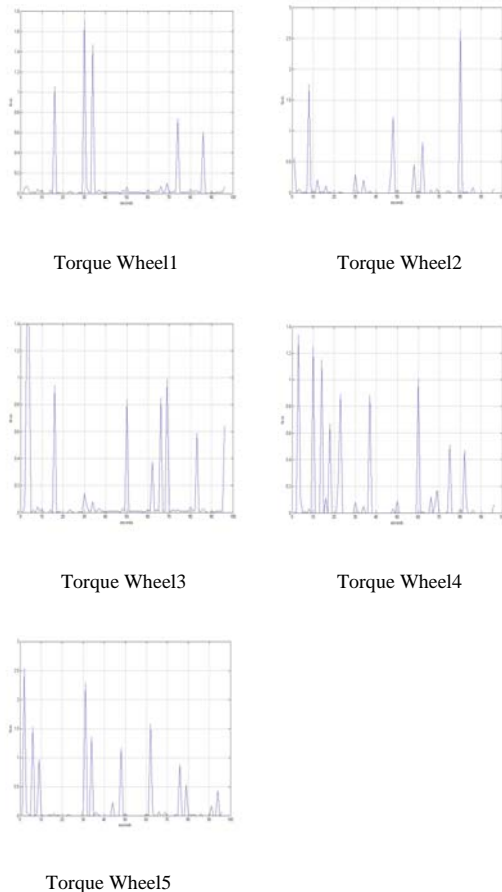


Figure13 plot of wheel motor torques in N-m

As can be seen from figure13 that the maximum torque requirement of the rover has increased to 2.6 N-m This follows from the fact that due to the complexity of the terrain there is corresponding increase in the amount of traction force required to maintain equilibrium of the system.

## 7 Conclusion and Future Work

In this paper we have proposed a new five wheeled passive suspension rover which is deduced from the current

existing suspension mechanism Shrimp by significantly reducing the number of joints and the number of wheels but yet maintaining a good terrain adaptability. The compliance added to the back wheel is an added novelty in the proposed mechanism. A quasi-static model for wheel motor torque control was presented. Uneven terrain simulations confirm the efficacy of the proposed mechanism. The future work is related to the development of the rover and analyzing path tracking capability of the rover in a fully 3D rough terrain.

## References

- [1] R. Volpe, J. Balaram, T. Ohm and R. Ivlev, "Rocky 7: A next generation mars rover prototype," *J. Advanced Robotics*, vol. 11, no. 4, pp. 341–358, Dec. 1997.
- [2] T. Estier, Y. Crausaz, B. Merminod, M. Lauria, R. Piguet, and R. Siegwart, "An innovative space rover with extended climbing abilities," in *Proc. Int. Conf. Robotics in Challenging Environments*, Albuquerque, USA, 2000.
- [3] Low Power Mobility System for Micro Planetary Rover "Micro5" in *Proc i-SAIRAS-99*, ESTEC Noorwidjijik, The NetherLands
- [4] "Lunokhod-1", FTD-MT-24-1022-71, pp.66-77.
- [5] A. Eremenko et al.: "Rover in The Mars 96 MISSION", Missions, Technologies and Design of Planetary Mobile Vehicles, pp.277-300, 1992.
- [6] Ashitava Ghosal, "Robotics –Fundamental Concepts and Analysis," First Edition, *Oxford University Press*.
- [7] M. Lauria, Y.Piguet and R.Siegwart, "Octopus: an autonomous wheeled climbing-robot", CLAWAR, 2002.
- [8] Vijay Prakash Eathakota, Arun Kumar Singh, Srikanth Kolachalama and K.Madhava Krishna in *Proc"18th IEEE-International Symposium On measurements and Control in Robotics"*, Sept. 2008 Bangalore, India.